# Hydrostatic and Geostrophic Adjustment in a Compressible Atmosphere: Initial Response and Final Equilibrium to an Instantaneous Localized Heating

JEFFREY M. CHAGNON AND PETER R. BANNON

*Department of Meteorology, The Pennsylvania State University, University Park, Pennsylvania*

(Manuscript received 15 March 2001, in final form 25 June 2001)

ABSTRACT

The initial and steady-state response of a compressible atmosphere to an instantaneous, localized heat source is investigated analytically. Potential vorticity conservation removes geostrophic and hydrostatic degeneracy and provides a direct method for obtaining the steady-state solution. The heat source produces a vertical potential vorticity dipole that induces a hydrostatically and geostrophically balanced cyclone–anticyclone structure in the final state. For a typical deep mesoscale heating, the net displacements required for the adjustment to the final steady state include a small, $O$(100 m) ascent of the core of the heated air with weak far-field descent and a large, $O$(10 km) outward/inward lateral displacement at the top/base of the heating.

The heating initially generates available elastic and potential energy. The energy is then exchanged between kinetic, elastic, potential, and acoustic and gravity wave energy. In the final state, after the acoustic and gravity wave energy has dispersed, the remaining energy is partitioned between kinetic, and available potential and elastic energy. The fraction of wave energy increases with increasing horizontal wavenumber.

The effect of several vertical boundary conditions is assessed. It is shown that a rigid lid suppresses the vertical expansion of the heated layer and reduces the fraction of wave energy. The impact of the rigid lid on the steady-state solution is maximized for the horizontal wavenumber zero solution and when the heating takes place close to the rigid upper boundary.

The compressible solution is used as a prototype for comparing and evaluating several compressibility approximations: the anelastic, pseudo-incompressible, and modified-compressible approximations. The anelastic model omits the available elastic energetics entirely, but the pseudo-incompressible and modified-compressible models omit either its generation or storage. The result is an ambiguous projection of heating energy onto the remaining energy terms. The errors associated with these approximations are only significant on synoptic scales. Furthermore, the modified-compressible set does not conserve potential vorticity globally.

The initial response to the heating differs for each approximation. Although the initial compressible response consists of pressure and potential temperature anomalies confined to the heated layer, the modified-compressible atmosphere generates density and potential temperature anomalies but no pressure anomaly. The anelastic atmosphere undergoes an instantaneous acoustic adjustment in which pressure and density anomalies exist inside and outside of the heated region. The pseudo-incompressible atmosphere generates an instantaneous, net divergence characterized by a residual velocity remaining after the heating and an instantaneous pulse in the pressure and velocity fields.

## 1. Introduction

Large-scale, midlatitude, atmospheric flows exhibit a tendency to be in hydrostatic and geostrophic balance. However, rapid, localized heat sources embedded in the synoptic-scale flow (e.g., mesoscale convective systems) can force the synoptic-scale flow away from hydrostatic and geostrophic balance. This imbalance is characterized by the creation of potential vorticity anomalies and the generation of a spectrum of buoyancy and acoustic waves. The unbalanced atmosphere adjusts toward a new hydrostatic and geostrophic state, determined by the magnitude and geometry of the potential vorticity anomaly. Blumen (1972) and Gill (1982) have reviewed the fundamental problem of the adjustment of a geophysical flow after an initial perturbation from a balanced state. Typically the initial perturbation is an addition of momentum or of mass. Most of the literature emphasizes the subsequent evolution of the flow toward a state of geostrophic balance, the time- and length scales of the adjustment, and the partitioning of the energy between the final steady state and the transients. In contrast, recent studies (Raymond 1986; Bretherton 1988, 1993; Bretherton and Smolarkiewicz 1989; Shutts and Gray 1994) indicate that considerable insight into the workings of moist convection can be gained by the examination of the response to prescribed heat sources.

This paper describes the hydrostatic and geostrophic

*Corresponding author address:* Peter R. Bannon, Department of Meteorology, The Pennsylvania State University, University Park, PA 16802.
E-mail: bannon@ems.psu.edu

adjustment to a prescribed, rapid, localized heating in a compressible atmosphere. The approach is analytic and holds for linearized dynamics. We focus on the initial response to the heating and the final steady-state equilibrium. From these solutions we infer the wave energetics during the process of adjustment and the net parcel displacements. We also assess the ability of several common approximations of the fully compressible equations to model the adjustment problem correctly. For example, the need to filter acoustic modes from model governing equations has led to the anelastic approximation [see Bannon (1996b) for a review and synthesis of these theories]. An attempt to relax the assumption of local incompressibility in the anelastic approximation has led to the pseudo-incompressible theory of Durran (1989). Another approximation commonly used in mesoscale modeling that retains both compressibility and numerical efficiency is the modified-compressible approximation (Klemp and Wilhelmson 1978). The present study also serves as an extension of the work of Bannon (1995a,b, 1996a) on hydrostatic adjustment to the fully three-dimensional problem.

Section 2 describes the compressible model of the three-dimensional hydrostatic and geostrophic adjustment process. Section 3 presents the compressible solutions. Section 4 presents an intercomparison of the anelastic, pseudo-incompressible, and modified-compressible approximations. Section 5 discusses the salient features of the adjustment process and the ability of these approximations to simulate the adjustment adequately.

## 2. The compressible model

### a. Governing equations

The governing equations for a compressible, dry, inviscid, rotating atmosphere on an $f$ plane in Cartesian coordinates linearized about an isothermal, resting base state are

$$\rho_s \frac{\partial u'}{\partial t} = -\frac{\partial p'}{\partial x} + \rho_s f v', \tag{2.1a}$$

$$\rho_s \frac{\partial v'}{\partial t} = -\frac{\partial p'}{\partial y} - \rho_s f u', \tag{2.1b}$$

$$\rho_s \frac{\partial w'}{\partial t} = -\frac{\partial p'}{\partial z} - \rho' g, \tag{2.1c}$$

$$\frac{\partial \theta'}{\partial t} + w' \frac{\partial \theta_s}{\partial z} = \dot{\Theta} \equiv \frac{\theta_s}{\rho_s C_p T_s} Q, \tag{2.1d}$$

$$\frac{\theta'}{\theta_s} = \frac{p'}{\gamma p_s} - \frac{\rho'}{\rho_s}, \tag{2.1e}$$

$$\frac{\partial \rho'}{\partial t} + \nabla \cdot (\rho_s \mathbf{u}') = 0, \tag{2.1f}$$

where $Q$ is the heating rate per unit volume, $g$ is the vertical acceleration due to gravity, $f$ is the constant Coriolis parameter, and $\gamma = c_p/c_v = 1.4$ is the ratio of the specific heats. A subscript $s$ denotes a static, base-state quantity, and a superscript prime denotes a perturbation from the base state. The base-state quantities are

$$T_s = T_*, \qquad p_s = p_* \exp(-z/H_s),$$
$$\rho_s = \rho_* \exp(-z/H_s), \qquad \theta_s = \theta_* \exp(\kappa z/H_s), \tag{2.2}$$

where $T_*$, $p_*$, $\theta_* = T_*$, and $\rho_*$ are constants satisfying the ideal gas law and Poisson's relation. Here, $\kappa = R/c_p$, and $H_s = RT_s/g$ is the density scale height in an isothermal atmosphere. The isothermal base state is an analytically convenient representation of a statically stable atmosphere. Note that the height $z = 0$ corresponds to a location in the midtroposphere, not the surface of the earth. The values of the parameters chosen for this study are representative of the *U.S. Standard Atmosphere* in the midtroposphere:

$$f = 10^{-4}\ \text{s}^{-1}, \qquad N_s = 0.0198\ \text{s}^{-1},$$
$$H_s = 7.32\ \text{km}, \qquad g = 10\ \text{m s}^{-2},$$
$$p_* = 540\ \text{hPa}, \qquad \rho_* = 0.738\ \text{kg m}^{-3},$$
$$T_* = 255\ \text{K}.$$

Equations (2.1a,b,c) are the momentum equations. Equations (2.1d,e,f) are the entropy equation, the linearized Poisson's relation, and the mass conservation equation, respectively.

The nonhydrostatic, ageostrophic, initial state is produced by a prescribed warming function of the form

$$\dot{\Theta} = \frac{\theta_s \Delta p}{\rho_s g H_s \gamma}[H(z + d) - H(z - d)]\delta(t)s(x, y), \tag{2.3}$$

where $H$ is the Heaviside step function, $d$ is the heating half depth, $\delta$ is the Dirac delta function, and $s$ is an arbitrary function describing the horizontal structure of the heating. Here $H$ and $s$ are dimensionless functions, and $\delta$ has dimensions inverse to those of its argument. The magnitude of the heating is specified by $\Delta p$, that is, the amplitude of the initial pressure perturbation. Before the heating is applied, all fields satisfy the base state. The initial conditions are thus

$$(u', v', w', p', \theta', \rho') = (0, 0, 0, 0, 0, 0), \quad \text{for } t < 0. \tag{2.4}$$

Solution of (2.1) also requires the specification of vertical boundary conditions. We consider three distinct conditions. The infinite atmosphere extends infinitely in both vertical directions, and the far-field pressure perturbation fields vanish. The semi-infinite atmosphere is characterized by a rigid surface placed below the heated layer at $z = -D = -6$ km where the vertical velocity is zero. The finite atmosphere is bounded both above and below the heated layer by rigid boundaries at $z =$

$\pm D$ where the vertical velocity is zero. The rigid boundary condition on the pressure field is

$$\frac{\partial p'}{\partial z} = -\frac{p'}{\gamma H_s}. \tag{2.5}$$

Equation (2.5) is derived by setting $w' = 0$ in (2.1c,d) and by applying the condition that, because there is no heating on the boundary, $\theta' = 0$ at the boundaries.

*b. Potential vorticity conservation*

The steady-state solution to (2.1) with (2.3) is obtained using the principle of potential vorticity conservation

$$\frac{\partial q'}{\partial t} = \frac{f}{\rho_s}\frac{\partial}{\partial z}\left(\frac{\rho_s g\dot{\Theta}}{\theta_s N_s^2}\right), \tag{2.6}$$

where the potential vorticity perturbation, $q'$, is

$$q' = \zeta' + f\left(\frac{\theta'}{\theta_s} - \frac{p'}{\gamma p_s}\right) + \frac{f}{\rho_s}\frac{\partial}{\partial z}\left(\frac{\rho_s g\theta'}{\theta_s N_s^2}\right), \tag{2.7}$$

and $\zeta'$ is the vertical component of the relative vorticity. The steady-state potential vorticity can be found by integrating (2.6) with respect to time. Using (2.3) we find

$$\begin{aligned} q_f' &= \int_0^\infty \left[\frac{f}{\rho_s}\frac{\partial}{\partial z}\left(\frac{\rho_s g\dot{\Theta}}{\theta_s N_s^2}\right)\right] dt \\ &= \frac{f\Delta p}{\rho_s N_s^2 \gamma H_s}[\delta(z+d) - \delta(z-d)]s(x, y), \end{aligned} \tag{2.8}$$

where the subscript $f$ denotes a final, steady-state quantity.

The potential vorticity anomaly generated by (2.3) is a vertical dipole. The global integral of the dipole anomaly is zero, and potential vorticity is thus globally conserved (Obukhov 1963). Using the hydrostatic and geostrophic relations, the steady-state form of (2.7) can be written in terms of the pressure perturbation as

$$\rho_s f q_f' = \left[\nabla_h^2 + \frac{f^2}{N_s^2}\left(\frac{\partial^2}{\partial z^2} + \frac{1}{H_s}\frac{\partial}{\partial z}\right)\right]p_f'. \tag{2.9}$$

Combining (2.8) and (2.9) yields an equation governing the steady-state pressure perturbation:

$$\begin{aligned} &\left[\frac{N_s^2}{f^2}\nabla_h^2 + \left(\frac{\partial^2}{\partial z^2} + \frac{1}{H_s}\frac{\partial}{\partial z}\right)\right]p_f' \\ &\quad = \frac{\Delta p}{\gamma H_s}[\delta(z+d) - \delta(z-d)]s(x, y). \end{aligned} \tag{2.10}$$

We can simplify (2.10) by applying a Fourier transform in $x$ and $y$,

$$P_f'(k, l, z) = \iint p_f'(x, y, z)e^{-ikx}e^{-ily}\, dx\, dy,$$

and by applying the vertical coordinate transformation defined by

$$\hat{P}_f(k, l, z) = P_f'(k, l, z)e^{z/2H_s},$$

to obtain

$$\begin{aligned} &\left(\frac{\partial^2}{\partial z^2} - \frac{1}{H_R^2}\right)\hat{P}_f \\ &\quad = \frac{\Delta p}{\gamma H_s}e^{z/2H_s}[\delta(z+d) - \delta(z-d)]S(k, l), \end{aligned} \tag{2.11}$$

where

$$H_R = \left[\frac{N_s^2}{f^2}(k^2 + l^2) + \frac{1}{4H_s^2}\right]^{-1/2},$$

and $S(k, l)$ is the Fourier transform of $s$. The compressible Rossby height, $H_R$, is the $e$-folding distance for the solutions to (2.11).

The Green's function procedure by which (2.11) is solved is presented in appendix A. We apply a numerical inverse fast Fourier transform to the solutions of (2.11) to obtain solutions in physical space. A Lanczos smoothing factor (Arfken 1970) is applied to the wind field in order to avoid convergence problems with the derivative of a Fourier series.

*c. Energetics*

The energy conservation equation, formed from (2.1), is

$$\begin{aligned} &\frac{\partial}{\partial t}\left[\frac{1}{2}\rho_s(u'^2 + v'^2 + w'^2) + \frac{\rho_s}{2N_s^2}\left(\frac{g\theta'}{\theta_s}\right)^2 + \frac{p'^2}{2\gamma p_s}\right] \\ &\quad = -\nabla\cdot(p'\mathbf{u}') + \dot{\Theta}\left[\frac{\rho_s}{N_s^2}\frac{g^2\theta'}{\theta_s^2} + \frac{p'}{\theta_s}\right]. \end{aligned} \tag{2.12}$$

The first term in the brackets on the left-hand side of (2.12) is the kinetic energy (KE) per unit volume, the second is the available potential energy (APE) per unit volume, and the third is the available elastic energy (AEE) per unit volume. The terms on the right-hand side are the wave energy flux convergence and the generation by heating, respectively. The generation term, shown in brackets on the right-hand side, is composed of two parts: the first produces available potential energy, and the second produces available elastic energy.

The kinetic energy, available elastic energy, and available potential energy equations are, respectively,

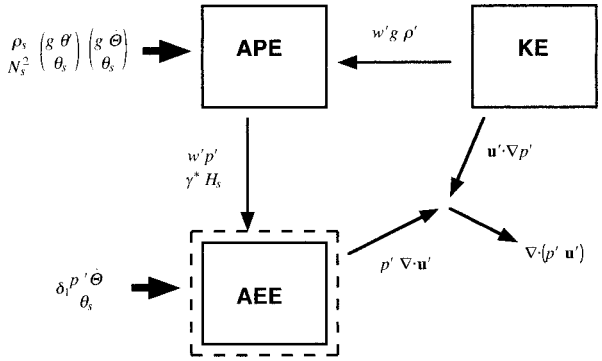


FIG. 1. Schematic illustration of the energy conversions between available potential (APE), available elastic (AEE), and kinetic energy (KE). Arrows indicate direction of positive energy conversion. The dashed box indicates that there is no storage of AEE if $\delta_2 = 0$. In the compressible atmosphere [$\delta_1 = 1$, $\delta_2 = 1$, $\gamma^* = \gamma$] there is diabatic generation and storage of AEE. The modified-compressible atmosphere [$\delta_1 = 0$, $\delta_2 = 1$, $\gamma^* = \gamma = 7/5$] ignores the generation of AEE. The pseudo-incompressible atmosphere [$\delta_1 = 1$, $\delta_2 = 0$, $\gamma^* = \gamma$] ignores the storage of AEE. The anelastic atmosphere [$\delta_1 = 0$, $\delta_2 = 0$, $\gamma^* = 1$] ignores both the storage and generation of AEE and ensures that the conversion of APE is consistent with the work done in squeezing an air parcel.

$$\frac{\partial}{\partial t}\left(\frac{1}{2}\rho_s\mathbf{u}'\cdot\mathbf{u}'\right) = -\mathbf{u}'\cdot\boldsymbol{\nabla}p' - w'\rho'g, \tag{2.13a}$$

$$\frac{\partial}{\partial t}\left(\frac{p'^2}{2\gamma p_s}\right) = -p'\boldsymbol{\nabla}\cdot\mathbf{u}' + \frac{p'\dot{\Theta}}{\theta_s} + \frac{w'p'}{\gamma H_s}, \tag{2.13b}$$

$$\frac{\partial}{\partial t}\left[\frac{\rho_s}{2N_s^2}\left(\frac{g\theta'}{\theta_s}\right)^2\right] = w'\rho'g - \frac{w'p'}{\gamma H_s} + \frac{\rho_s}{N_s^2}\left(\frac{g\theta'}{\theta_s}\right)\left(\frac{g\dot{\Theta}}{\theta_s}\right). \tag{2.13c}$$

The heating provides an instantaneous source of available elastic and available potential energy. Energy is then converted between available potential and kinetic energy by the work done by the buoyancy force, $w'\rho'g$, and between available elastic and available potential energy by the work done against the pressure, $w'p'/(\gamma H_s)$. Figure 1 presents a schematic of the energetics.

## 3. Compressible solution

We consider the response in a compressible atmosphere to a two-dimensional heating with horizontal structure given by

$$s(x, y) = \frac{a^2}{x^2 + a^2}, \tag{3.1}$$

where $a$ determines the horizontal half-width of the heating function. The perturbation fields of density, potential temperature, and velocity are normalized by

$$\Delta\rho = \frac{\Delta p}{gH_s}, \qquad \Delta\theta = \frac{\Delta pT_s}{p_*}, \qquad \Delta V = \frac{\Delta p}{\rho_* f a}, \tag{3.2}$$

respectively. For an initial pressure perturbation $\Delta p$ of 7.38 hPa, these scales are $1 \times 10^{-2}$ kg m$^{-3}$, 3.5 K, and 100 m s$^{-1}$, respectively.

### a. Initial response

The compressible form of the mass conservation equation (2.1f), integrated about an infinitesimal region in time containing $t = 0$, with (2.4), implies that the density perturbation immediately after the heating (denoted by a subscript $+$) is zero:

$$\rho'(t = 0_+) \equiv \rho'_+ = 0. \tag{3.3}$$

Integration of (2.1a,b,c) in time implies that there is no initial velocity field:

$$(u'_+, v'_+, w'_+) = (0, 0, 0). \tag{3.4}$$

Equation (2.1d), with (2.3), (2.4), and (3.4) implies an initial potential temperature perturbation of the form

$$\theta'_+ = \frac{\theta_s\Delta p}{\rho_s g H_s\gamma}[H(z + d) - H(z - d)]s(x, y). \tag{3.5}$$

Equation (2.1e) with (3.3) and (3.5) implies an initial pressure perturbation of the form

$$p'_+ = \Delta p[H(z + d) - H(z - d)]\, s(x, y). \tag{3.6}$$

Thus the initial response to an instantaneous heating involves no motion nor density anomaly, but nonzero pressure and potential temperature perturbations confined to the region of heating.

Figures 2a and 2b present the initial potential temperature and pressure fields, where the half-width of the heating function is $a = 100$ km. The horizontal axis is scaled by the Rossby radius of deformation,

$$L_R = 2d\frac{N_s}{f}. \tag{3.7}$$

For the parameters prescribed in this study with $d = 5$ km, the Rossby radius is 1890 km. The initial potential temperature and pressure fields are confined vertically to the heated layer, and decay horizontally according to (3.1). The vertical structure of the initial potential temperature is the same as that of the warming rate, $\dot{\Theta}$, which increases with height because the base-state density field decays with height. The vertical structure of the initial pressure is the same as that of the heating rate per unit volume, $Q$, which is constant.

### b. Steady-state fields

Figure 3 presents the steady-state perturbation pressure, density, potential temperature, and velocity fields for the infinite atmosphere. The initial potential vorticity anomaly (2.8) is created by the heating function (2.3) whose horizontal structure is given by (3.1) with $a = 100$ km. This vertical potential vorticity dipole determines the structure of the steady state. The dipole is

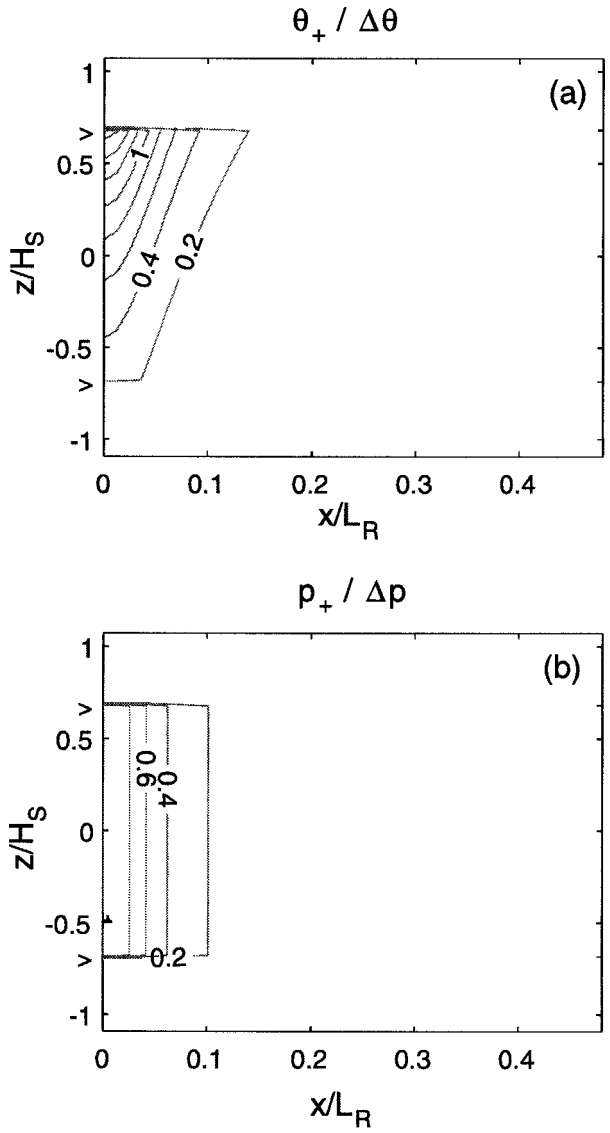


FIG. 2. Initial perturbation field for (a) potential temperature and (b) pressure in an infinite, compressible atmosphere. The vertical axis is scaled by the density scale height, $H_s$; the horizontal axis is scaled by the Rossby radius of deformation, $L_R$. Here and in subsequent figures, dashed/solid lines indicate negative/positive contours and a symbol ''>'' on the ordinate indicates the height of the potential vorticity anomalies.

characterized by a cyclone/anticyclone located below/above the initially warmed layer. A vertical asymmetry exists in this structure due to the exponential decay of the base-state density. The magnitude of the pressure perturbation associated with this feature decays with horizontal distance from the heating center. The existence of the low-level cyclone implies a net loss of mass in the vertical column near the heating center because the steady state is in hydrostatic balance. Such a feature does not exist in the horizontally homogeneous adjustment problem (Bannon 1995a).

The adjustment from the initial to the final state involves a redistribution of mass. The net horizontal displacement, $\Delta x$, is derived by integration of the $y$ momentum equation (2.1b) from $t = 0_+$ to $t \to \infty$. The net vertical displacement, $\Delta z$, is derived by integration of the adiabatic form of the heat equation (2.1d) from $t = 0_+$ to $t \to \infty$. We find

$$\Delta x = -\frac{1}{f} v_f, \qquad \Delta z = -\frac{(\theta_f - \theta_+)}{\dfrac{d\theta_s}{dz}}. \tag{3.8}$$

The total displacement vector is defined as $\Delta \mathbf{s} = (\Delta x, \Delta z)$. The $x$ and $z$ components are normalized by

$$\Delta d_x = \frac{\Delta p}{\rho_s f N_s a}, \qquad \Delta d_z = \frac{\Delta p g}{p_* N_s^2}. \tag{3.9}$$

Note that the $x$ normalization increases with height like $\exp(z/Hs)$. At $z = 0$ with $\Delta p = 7.38$ hPa the displacements are $\Delta d_x = 5.05$ km and $\Delta d_z = 348$ m.

Figure 4 displays the normalized displacement vectors:

$$\Delta \hat{\mathbf{s}} = \left( \frac{\Delta x}{\Delta d_x}, \frac{\Delta z}{\Delta d_z} \right). \tag{3.10}$$

Because the $x$ displacement normalization is inversely proportional to the base-state density, the amplitude of the $x$ component of the normalized displacement vectors is less dependent on $z$ than the scaled velocity field. The horizontal displacement vectors indicate flow away from the top of the heated column and flow toward the bottom of the heated column. Upward vectors exist in the heated column, with weaker compensating subsidence outside of this region, and a weak low-level return flow directed toward the heated column.

The structure of the steady-state fields reflects the net displacements. The positive density anomaly immediately above the heated layer reflects the net upward expansion of the heated layer into the adjacent atmosphere. A corresponding feature is apparent in the potential temperature field. A negative potential temperature perturbation exists immediately above the heated layer, reflecting the net upward advection of lower, base-state values of potential temperature. The positive density anomaly immediately below the heated layer is the result of the return flow at low levels. The geostrophically balanced velocity anomaly at low levels is another indication of this return flow.

### c. Effects of vertical boundaries

Figures 5 and 6 illustrate the effect of vertical boundaries on the steady-state pressure field and net displacements, respectively. In the semi-infinite atmosphere, the negative pressure perturbation at low levels is much stronger and broader than that in the infinite atmosphere (Fig. 5a). This feature corresponds to the enhancement of the low-level inflow in the semi-infinite atmosphere

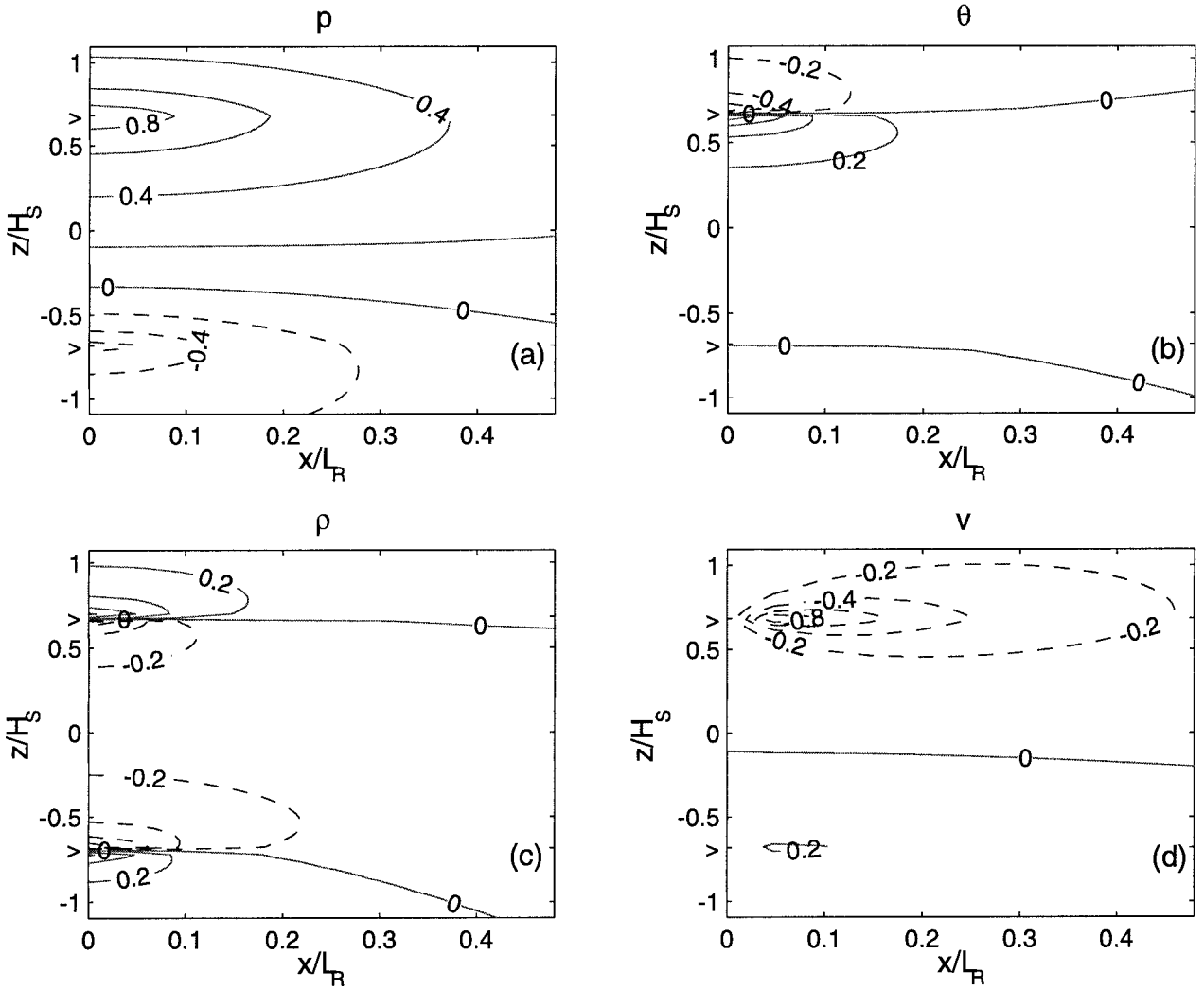


FIG. 3. Steady-state, perturbation field for (a) pressure, (b) potential temperature, (c) density, and (d) velocity in a compressible infinite atmosphere. Each field is normalized by its maximum value of $0.048\Delta p$, $0.265\Delta\theta$, $0.106\Delta\rho$, $0.014\Delta V$, respectively. The heating half-width is $a = 100$ km; the half-depth is $d = 5$ km.

(Fig. 6a). In contrast, the vertical displacement field is diminished.

In the finite atmosphere, the positive pressure perturbation at high levels is much larger and broader than in either the semi-infinite or infinite atmosphere (Fig. 5b). The rigid upper boundary suppresses the net upward expansion of the heated layer but the horizontal displacement vectors are enhanced in the finite atmosphere, relative to the semi-infinite atmosphere. This effect is most pronounced for the lowest horizontal wavenumber modes whose Rossby heights, $H_R$, are large.

### *d. Effects of heating geometry*

The effect of the heating function's aspect ratio on the structure of the steady-state pressure field is presented in Fig. 7 for an infinite atmosphere. (We note that the Rossby radius is a function of heating half-depth and thus the scaling of the horizontal axis is variable for each panel.) We define the aspect ratio as $\delta = d/a$, where $a$ is the horizontal decay half-width of the heating function $s$ and $d$ is its vertical half-depth [defined in Eq. (2.3)]. We present results for aspect ratios $\delta = 50^{-1}$, $20^{-1}$, $5^{-1}$, and $2^{-1}$. The locations of the pressure perturbation maxima and minima coincide with the location of maximum and minimum potential vorticity anomalies. A continuous transition in the geometry of the steady-state solution is not observed as the aspect ratio is varied smoothly. Rather, it is more appropriate to consider the transition of the solution geometry as the depth scale is held constant and the horizontal scale is varied, and vice versa. For example, decreasing the heating half-depth while holding $a$ constant produces wider and flatter structures with larger amplitude (compare Fig. 7a with Fig. 7c and Fig. 7b with Fig. 7d).

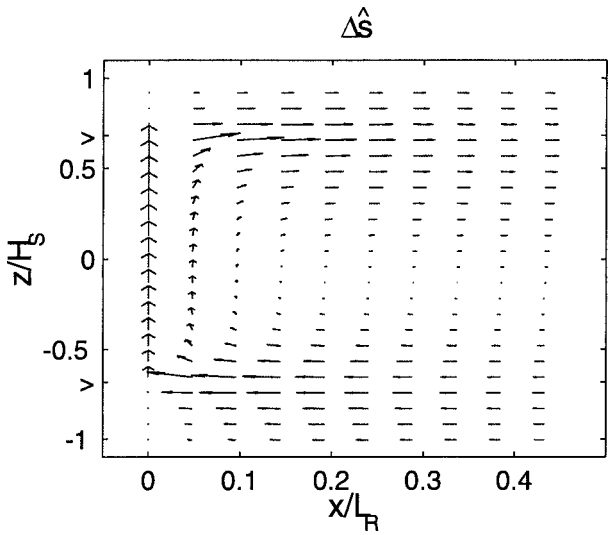


FIG. 4. Normalized displacement vectors for an infinite, compressible atmosphere. A vector whose length is one grid spacing in $x$ is equal to $\Delta d_x$; that in $z$ is $\Delta d_z$. Note that the normalization increases with height for the horizontal displacement vector. For example, the horizontal displacement is a factor of 3.92 greater at the top of the heating than at its base.

*e. Energetics*

For the initial response to the heating, there is no kinetic energy and the total energy is distributed between the available potential and elastic energies. We find

$$\mathrm{AEE}_i = \int_V \frac{p'^2}{2\gamma p_s}\, dV = \int \frac{\Delta p^2 [H(z+d) - H(z-d)] s^2(x,y)}{2\gamma p_s}\, dV,$$

$$\mathrm{APE}_i = \int_V \left(\frac{\rho_s}{2N_s^2}\right)\left(\frac{g\theta'}{\theta_s}\right)^2 dV = \frac{1}{\kappa\gamma}\mathrm{AEE}_i. \qquad (3.11)$$

The initial available elastic energy is a fraction $\kappa = R/c_p = 28\%$ of the total energy; the remainder is available potential energy. This distribution holds for all wavelengths.

For the steady state, each of the energy terms (AEE, APE, and KE) is calculated directly. The total energy in the final state is less than that in the initial. The difference is energy lost to the acoustic and gravity waves. Figure 8 presents the energetics as a function of horizontal wavelength, $\lambda = 2\pi/k$. We refer to this as the ''white noise'' spectrum, because each of the steady-state, vertically integrated energy terms in (2.12) is calculated at a particular wavenumber k and is normalized by the total energy residing in that wavenumber initially. This method removes the total energy dependence on heating half-width $a$ and is hence identical to the response from a white noise forcing. We note that scales larger than the circumference of the earth in Fig. 8 are an artifact of the analytic method and the use of an $f$ plane.

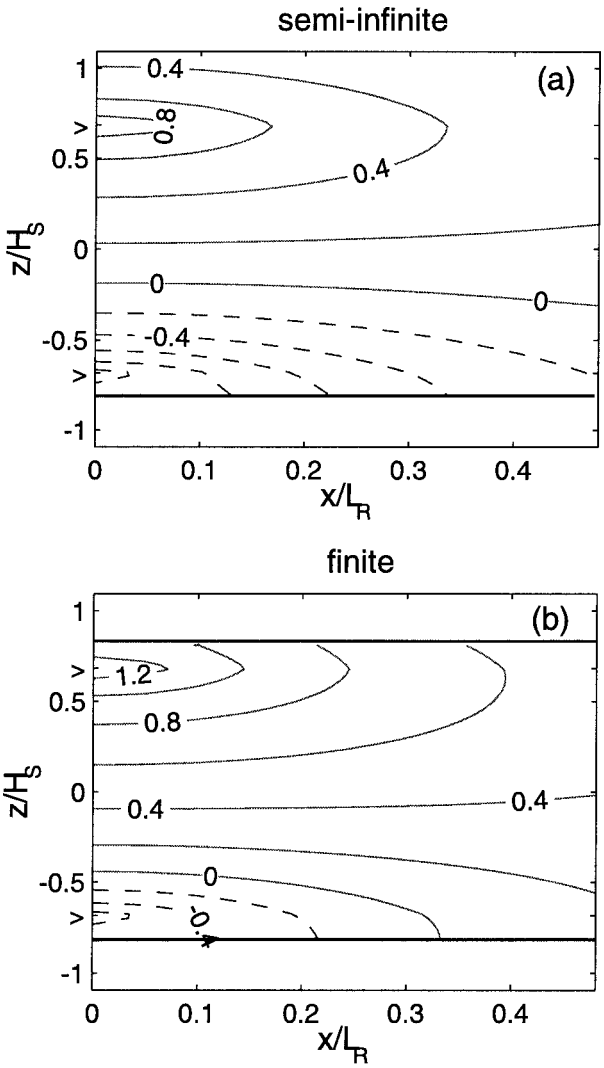


FIG. 5. Steady-state, pressure perturbation for (a) the semi-infinite and (b) the finite compressible atmosphere. The fields are normalized by the absolute maximum value in the infinite-atmosphere case (0.048 $\Delta p$). The heating half-width is $a = 100$ km; the half-depth is $d = 5$ km. The horizontal lines denote the location of the boundaries.

The large-wavelength limit in Fig. 8a gives the same partitioning as that in the 1D, acoustic adjustment problem (Bannon 1995a). This limit represents the case in which the heating is horizontally homogeneous and the adjustment occurs entirely in the vertical. There is no kinetic energy; a fraction $\kappa = 28\%$ of the total energy generates waves and the remaining energy is partitioned between the available elastic and potential energies. This large-wavelength limit corresponds to an initial heating with aspect ratio $\delta$ approaching zero. As $\lambda$ decreases (i.e., as $\delta$ increases) this fraction of wave energy monotonically increases, but the fraction of energy attributed to elastic and potential energy decreases. The fraction of kinetic energy increases as $\lambda$ decreases and

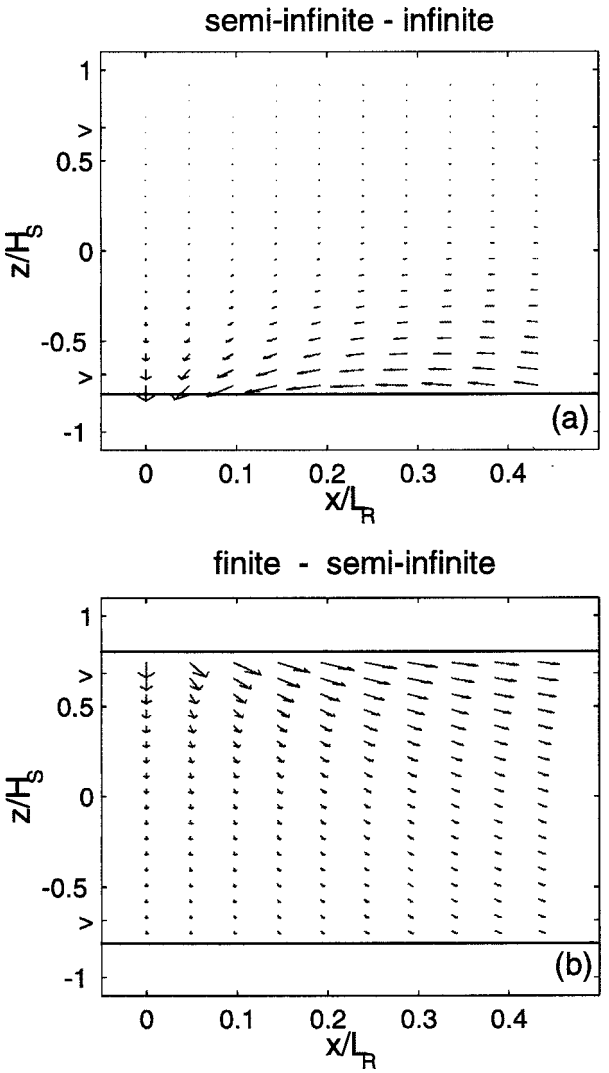


FIG. 6. Displacement vectors for (a) the semi-infinite and (b) the finite compressible atmosphere. The semi-infinite vectors are plotted as a deviation from the infinite atmosphere. The finite vectors are plotted as a deviation from the semi-infinite atmosphere. The $x$ and $z$ components are scaled by their respective maximum values: 0.55 $\Delta d_x$ and 0.029 $\Delta d_z$ in (a), and 0.44 $\Delta d_x$ and 0.063 $\Delta d_z$ in (b).

reaches a maximum near $\lambda \approx 7200$ km. At smaller length scales, the fraction of elastic energy is negligible. Available elastic energy is only significant at very large (synoptic) scales. For smaller scales, the wave energetics dominate and all the steady-state perturbations rapidly asymptote to zero.

This wavenumber dependence of the energetics has the following interpretation. For a small horizontal-scale heating, the mass adjustment occurs relatively quickly in the horizontal and the effects of Coriolis deflection are negligible. Consequently, all of the steady-state perturbation fields and energies are small. As the horizontal scale of the heating increases into the synoptic range, Coriolis deflection becomes increasingly significant. At these synoptic scales, the steady state is characterized by larger horizontal pressure perturbations, geostrophic velocity, and kinetic energy. Larger quantities of available potential and elastic energy also exist in the steady state due to the restriction of the horizontal mass adjustment by geostrophic motions. As the horizontal scale increases beyond the synoptic range, horizontal accelerations are reduced by the decreasing horizontal pressure gradients of the initial state. At these very large scales, the steady state is characterized by smaller horizontal pressure perturbations, geostrophic velocity, and kinetic energy. The degree to which horizontal mass adjustment occurs continues to decrease, and the steady-state available potential and elastic energy continues to increase.

TABLE 1. The amplitude and wavelength of the kinetic energy maximum as a function of the heating half-depth, $d$, in the infinite, semi-infinite, and finite compressible atmospheres. The amplitude is expressed as a fraction of the initial energy residing in that wavelength. The wavelength is given in parentheses in units of $10^3$ km. Here $D = 6$ km for the semi-infinite and finite atmospheres.

| $d$ (km) | Infinite | Semi-infinite | Finite |
|---|---|---|---|
| 1 | 0.11 (1.4) | 0.11 (1.4) | 0.11 (1.4) |
| 3 | 0.11 (4.4) | 0.13 (4.4) | 0.16 (4.6) |
| 5 | 0.12 (7.2) | 0.13 (5.3) | 0.18 (4.6) |
| 5.5 | 0.12 (7.9) | 0.13 (5.6) | 0.17 (4.6) |
| 5.9 | 0.13 (7.9) | 0.13 (5.6) | 0.17 (4.6) |

Figure 8 also describes the effect of vertical boundary conditions on the energetics. At large wavelengths the energetics of the semi-infinite atmosphere (Fig. 8b) is exactly equal to that for the infinite atmosphere. This behavior reflects the fact that the energetics in Lamb's hydrostatic adjustment problem are unaffected by a rigid lower boundary. At smaller wavelengths, the major effect of the boundary is to shift the peak in the kinetic energy to a wavelength of about 5300 km.

The finite-atmosphere energetics are characterized by suppressed wave generation at large wavelengths. The existence of rigid boundaries above and below the heated layer suppresses the vertical expansion of the heated layer and the generation of acoustic waves. The available potential and elastic energies become larger at larger wavelengths, but the kinetic energy maximum is increased and shifted to smaller scales ($\lambda \sim 4600$ km).

Table 1 presents the effect of the vertical boundaries and the heating half-depth, $d$, on the amplitude and wavelength of the kinetic energy maximum. The amplitude increases with increasing $d$. Although this increase is monotonic in the infinite atmosphere, it is not monotonic when the heating occurs very close to a boundary. The finite atmosphere produces the largest maximum, independent of $d$. The wavelength of this maximum increases monotonically with increasing $d$. However, the rate of increase is not the same in each atmosphere. The wavelength of the maximum is larger when boundaries are present for small heating half-

depth ($d < 5$ km) and is smaller for large heating half-depth ($d \geq 5$ km).

## 4. Comparison of anelastic, pseudo-incompressible, and modified-compressible approximations

### a. Governing equations

The linear geostrophic and hydrostatic adjustment problem presented in sections 2 and 3 provides a prototype problem for comparing and evaluating the pseudo-incompressible, modified-compressible, and anelastic sets of equations. A generalized set is formed by rewriting the linearized Poisson's relation (2.1e) and the mass conservation equation (2.1f) as

$$\frac{\theta'}{\theta_s} = \frac{p'}{\gamma^* p_s} - \frac{\rho'}{\rho_s}, \tag{4.1a}$$

$$\nabla \cdot \mathbf{u}' = \frac{w'}{\gamma^* H_s} + \delta_1 \frac{\dot{\Theta}}{\theta_s} - \delta_2 \frac{1}{\gamma^* p_s} \frac{\partial p'}{\partial t}, \tag{4.1b}$$

respectively. Equations (2.1a,b,c,d), with (4.1a,b), form a set of governing equations that includes each of the compressibility approximations. These approximations can be switched on/off through the three flags $\delta_1$, $\delta_2$, and $\gamma^*$ as follows:

$$\begin{aligned}
&\delta_1 = 1, \quad \delta_2 = 1, \quad \gamma^* = \frac{7}{5} \Rightarrow \text{compressible} \\
&\delta_1 = 0, \quad \delta_2 = 0, \quad \gamma^* = 1 \Rightarrow \text{anelastic} \\
&\delta_1 = 1, \quad \delta_2 = 0, \quad \gamma^* = \frac{7}{5} \Rightarrow \text{pseudo-incompressible} \\
&\delta_1 = 0, \quad \delta_2 = 1, \quad \gamma^* = \frac{7}{5} \Rightarrow \text{modified compressible.}
\end{aligned} \tag{4.2}$$

A similar notation was introduced by Durran (1989). Note that in (4.1a), $\gamma^*$ is treated as a flag for the anelastic approximation and may not satisfy the typical relationships for the ratio of specific heat capacities. We still denote $\gamma = c_p/c_v = 1.4$ as the ratio of specific heat capacities. For all but the anelastic approximation, $\gamma^* = \gamma$. In this section, we consider the response of the anelastic, pseudo-incompressible, and modified-compressible atmospheres to the instantaneous heating, (2.3), with horizontal structure (3.1). We apply the infinite atmosphere boundary condition and the initial conditions (2.4).

### b. Initial response

In the anelastic atmosphere, acoustic adjustment occurs instantaneously (Bannon 1995b). The anelastic initial response is thus expected to deviate from the compressible initial response. Indeed, differences in the initial responses between the anelastic and compressible solutions provide insight into the nature and the extent of the acoustic adjustment. As in the compressible atmosphere, (2.1a)–(2.1c) imply no initial velocity and (3.4) holds in the anelastic atmosphere. Since the anelastic form of the heat equation, (2.1d), is identical to the compressible form, (3.5) also holds in the anelastic atmosphere. Using the anelastic form of (4.1a) and (2.1a)–(2.1c) to rewrite the anelastic form of (4.1b), a diagnostic equation for the anelastic pressure field is derived:

$$\left(\nabla^2 + \frac{1}{H_s}\frac{\partial}{\partial z}\right)p' = \rho_s f \zeta' + g\frac{\partial}{\partial z}\left(\frac{\rho_s}{\theta_s}\theta'\right). \tag{4.3}$$

Evaluated with (3.4) and (3.5), and Fourier transformed, (4.3) yields

$$\left[\frac{d^2}{dz^2} - \left(k^2 + l^2 + \frac{1}{4H_s^2}\right)\right]\hat{P}_+ = \frac{\Delta p}{\gamma H_s} e^{z/2H_s}[\delta(z + d) - \delta(z - d)]S(k, l). \tag{4.4}$$

Equation (4.4) is very similar to the equation governing the final state anelastic pressure [see section 4c and Eq. (4.10)]. The subtle difference between the anelastic final state and initial response is a factor of $N_s^2/f^2$ associated with the vertical decay scale for a particular Fourier mode. This difference represents the effects of the buoyancy adjustment process.

Figure 9b presents a plot of the initial anelastic pressure. Its amplitude is approximately 70% smaller than the compressible one and its structure exhibits a positive pressure perturbation above the heated layer and a small, negative perturbation below the heated layer. These differences reflect the effects of the acoustic adjustment.

Figure 9d presents a plot of the initial anelastic density field, found from (4.1a). Unlike the compressible atmosphere, the anelastic atmosphere produces a nonzero initial density perturbation that is negative in the heated layer, and positive above and below the heated layer. Again this structure is achieved entirely by the acoustic adjustment.

As in the compressible and anelastic atmospheres, the modified-compressible atmosphere must satisfy (3.4) and (3.5); thus there is no initial motion and the initial potential temperature is implied directly by (2.1d). The modified-compressible form of the mass conservation equation (4.1b) implies, upon integration about an infinitesimal region in time containing $t = 0$,

$$p'_+ = 0. \tag{4.5}$$

The initial modified-compressible density field is, applying (3.5) and (4.5) to (4.1a),

$$\rho'_+ = -\frac{\Delta p}{g H_s \gamma}[H(z + d) - H(z - d)]S(k, l). \tag{4.6}$$

Thus, in contrast to the compressible atmosphere, the modified-compressible atmosphere generates no initial

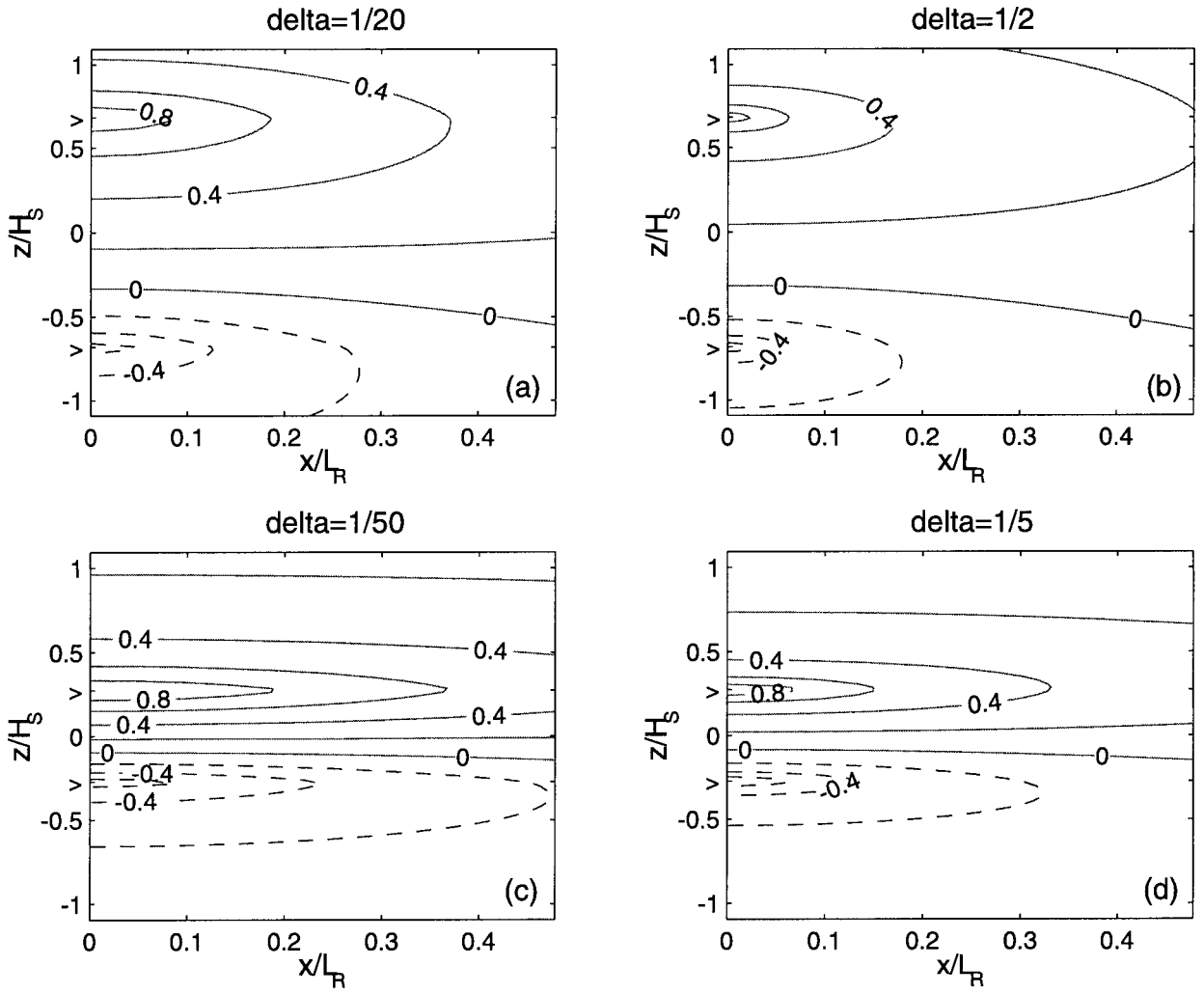


FIG. 7. Steady-state pressure perturbation field for the heating aspect ratio (a) $\delta = 1/20$, (b) $\delta = 1/2$, (c) $\delta = 1/50$, and (d) $\delta = 1/5$ in a compressible infinite atmosphere. The heating half depth, $d$, is 5 km in (a) and (b) but 2 km in (c) and (d). Each field is normalized by its maximum amplitude of $0.048\Delta p$, $0.0077\Delta p$, $0.037\Delta p$, and $0.004\Delta p$ for $\delta = 1/20$, 1/2, 1/50, and 1/5, respectively.

pressure response and a negative density response. Figure 9c plots this initial density field. Analogous to the initial compressible pressure field, the modified-compressible density field is constant with height in the heated layer and zero outside of the heated layer. The instantaneous production of this density anomaly implies a hydrostatic (but not a geostrophic) initial imbalance in the modified-compressible atmosphere.

The pseudo-incompressible initial response is more complicated. In the other cases, we made the implicit assumption that the fields are bounded at $t = 0$. This assumption allows the elimination of terms upon temporal integration about infinitesimal regions. However, this assumption is invalid for the pseudo-incompressible atmosphere because (4.1b) implies that there must be a net divergence during the heating. The solution of the pseudo-incompressible initial response is outlined in Appendix B.

*c. Potential vorticity conservation and steady-state fields*

The generalized potential vorticity equation is

$$\frac{\partial q'}{\partial t} = \frac{fg}{N_s^2\theta_s}\left\langle \frac{\partial}{\partial z} - \left[1 + \delta_1\left(\frac{\gamma^* - 1}{\gamma^*}\right)\right]\frac{1}{H_s}\right\rangle \dot{\Theta}, \quad (4.7)$$

where

$$q' = \zeta' + \frac{fg}{N_s^2\theta_s}\left(\frac{\partial}{\partial z} - \frac{1}{H_s}\right)\theta' - \delta_2\frac{f}{\gamma^* p_s}p'. \quad (4.8)$$

The final state potential vorticity is

$$q'_f = \frac{\Delta p f}{\gamma H_s N_s^2 \rho_s}\left[\left(\frac{\gamma^* - 1}{\gamma^*}\right)\frac{(1 - \delta_1)}{H_s}H^*(z, d) + \delta^*(z, d)\right]s(x, y), \quad (4.9)$$

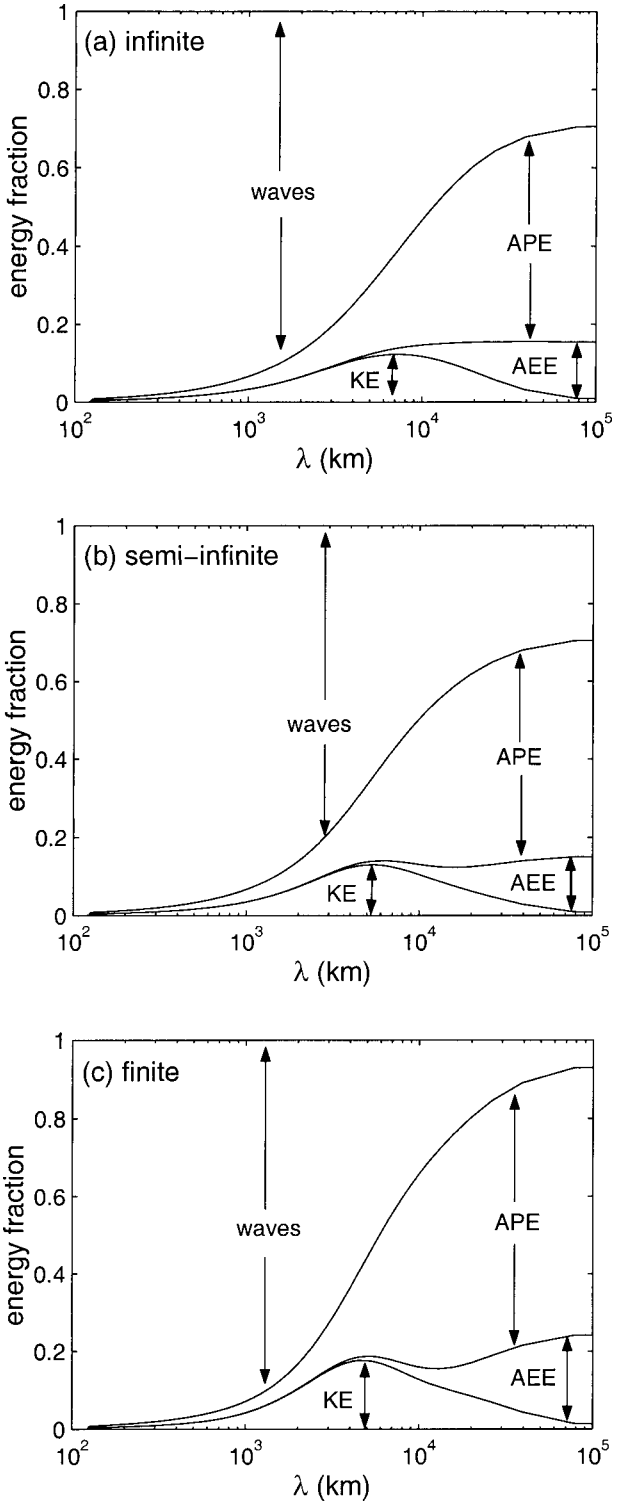


FIG. 8. Steady-state energetics for (a) the infinite, (b) the semi-infinite, and (c) the finite compressible atmosphere as a function of wavelength.

where $H^*(z, d) = H(z + d) - H(z - d)$ and $\delta^*(z, d) = \delta(z + d) - \delta(z - d)$. The final state potential vorticity is identical in the anelastic, pseudo-incompressible, and compressible atmospheres. There is a potential vorticity dipole that conserves potential vorticity globally. For the modified-compressible atmosphere [$\delta_1 = 0$, $\delta_2 = 1$, $\gamma^* = \gamma$] there is, in addition to the dipole, a potential vorticity monopole, the $H^*$ term, that violates the requirement that the potential vorticity be globally conserved (Obukhov 1963).

The equation governing the vertically and Fourier transformed final state pressure, corresponding to (4.8) and (4.9), is

$$\left(\frac{\partial^2}{\partial z^2} - C^2\right)\hat{P}_f = \frac{\Delta p}{\gamma H_s} e^{z/2H_s} S(k, l) \times \left[\left(\frac{\gamma^* - 1}{\gamma^*}\right)\frac{(1 - \delta_1)}{H_s} H^*(z, d) + \delta^*(z, d)\right], \quad (4.10)$$

where

$$C^2 = \frac{1}{H_R^2} - \left(\frac{\gamma^* - 1}{\gamma^*}\right)\frac{(1 - \delta_2)}{H_s^2}.$$

The analytical solutions to (4.10) for each set of equations are listed in Table A1.

Figure 10 presents the steady-state pressure perturbation fields for two of the compressibility approximations. The anelastic steady-state pressure perturbation field is not shown, because it is identical to the compressible solution (see Fig. 3a). In addition, the structure of the anelastic steady-state density and velocity perturbation fields is also identical to the compressible solution. However, the anelastic steady-state potential temperature field is, generally, larger than that of the compressible solution (Bannon 1995b). The modified-compressible steady-state pressure perturbation field is characterized by an anomalously weak anticyclone aloft and an anomalously strong, broad, low-level cyclone. Since this solution is equal to the sum of the compressible solution plus a contribution from the potential vorticity monopole, these errors are due to the monopole. The pseudo-incompressible approximation produces a steady-state pressure perturbation field characterized by an anomalously narrow and weak low-level cyclone, and a slightly stronger upper-level anticyclone. Since these errors exhibit very little structure in the horizontal direction, it suggests that they are most significant at very low horizontal wavenumber. Appendix A indicates that this approximation decreases the vertical decay scale associated with any particular horizontal Fourier mode and that this shift is maximized at zero wavenumber. Thus the errors associated with the pseudo-incompressible approximation are confined to low wavenumbers.

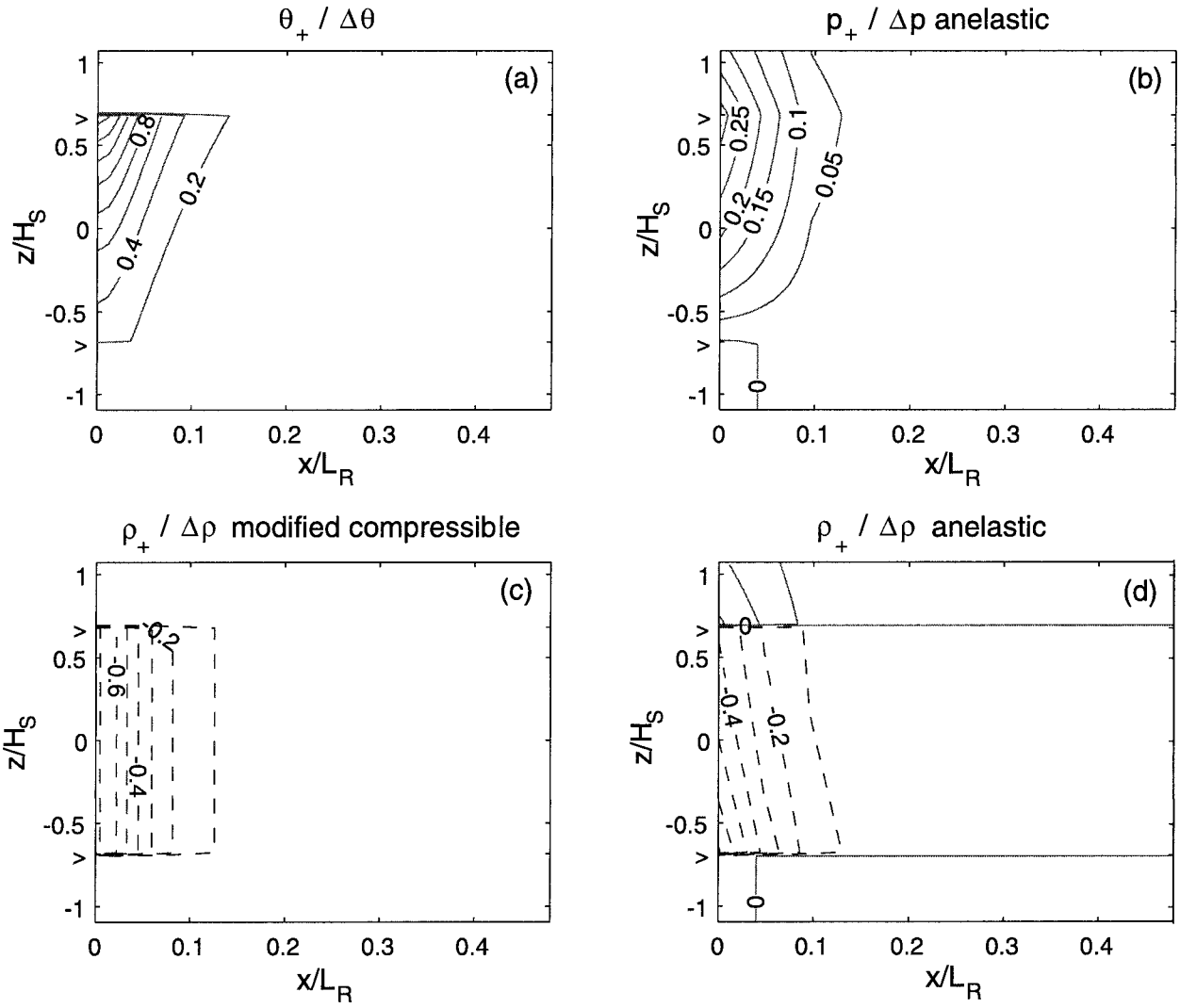


FIG. 9. Initial field for (a) potential temperature, (b) anelastic pressure, (c) modified-compressible density, and (d) anelastic density. The heating half-width is $a = 100$ km; the half-depth is $d = 5$ km.

*d. Energetics*

The generalized kinetic, available elastic, and available energy equations are

$$\frac{\partial}{\partial t}\left(\frac{1}{2}\rho_s \mathbf{u}' \cdot \mathbf{u}'\right) = -\mathbf{u}' \cdot \nabla p' - w'\rho' g, \tag{4.11a}$$

$$\delta_2 \frac{\partial}{\partial t}\left(\frac{p'^2}{2\gamma^* p_s}\right) = -p'\nabla \cdot \mathbf{u}' + \delta_1 \frac{p'\dot{\Theta}}{\theta_s} + \frac{w'p'}{\gamma^* H_s}, \tag{4.11b}$$

$$\frac{\partial}{\partial t}\left[\frac{\rho_s}{2N_s^2}\left(\frac{g\theta'}{\theta_s}\right)^2\right] = w'\rho' g - \frac{w'p'}{\gamma^* H_s} + \frac{\rho_s}{N_s^2}\left(\frac{g\theta'}{\theta_s}\right)\left(\frac{g\dot{\Theta}}{\theta_s}\right), \tag{4.11c}$$

respectively. Figure 1 depicts the balance in (4.11) schematically. The differences between the energy conservation relationships is in the treatment of the perturbation available elastic energetics, (4.11b). The anelastic approximation [$\delta_1 = 0$, $\delta_2 = 0$, $\gamma^* = 1$] removes elastic energy from the energy balance and contains no projection of the heating onto AEE. In spite of removing AEE from the balance, the resulting anelastic energy equation is consistent, because (4.11b) reduces to the anelastic continuity equation,

$$\nabla \cdot \mathbf{u}' - \frac{w'}{H_s} = 0.$$

The pseudo-incompressible balance [$\delta_1 = 1$, $\delta_2 = 0$, $\gamma^* = \gamma$] retains the generation of available elastic energy by the heating but removes its storage. The remaining two terms in (4.11b) must instantly balance the AEE generation. For $t > 0$, the balance involves only conversion between available potential and kinetic energy, and wave flux divergence. The available elastic energy plays no part in the pseudo-incompressible bal-

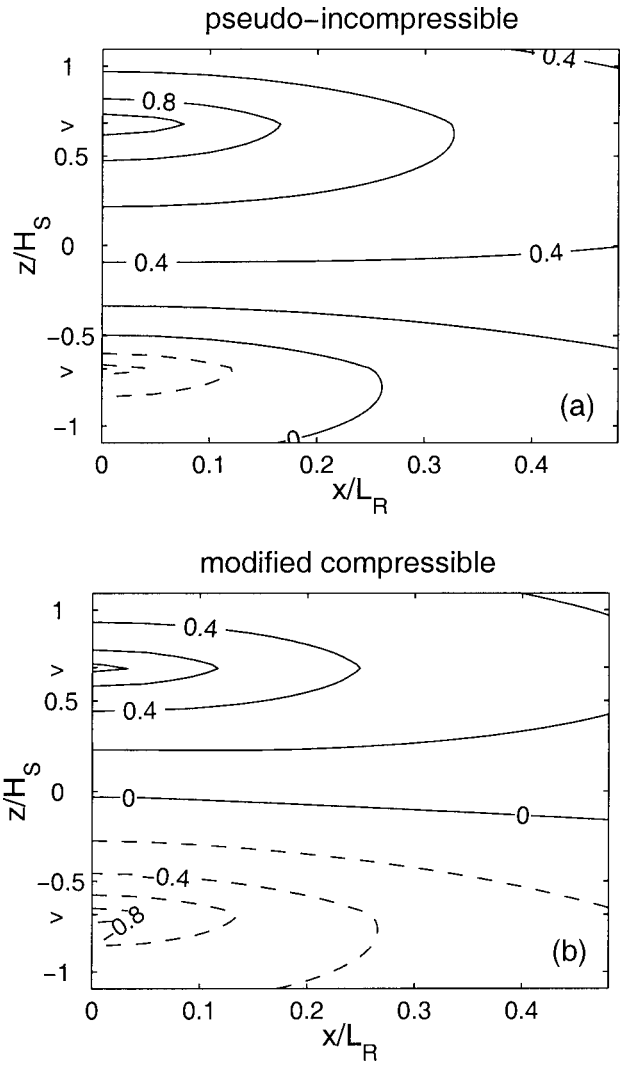


FIG. 10. Steady-state, pressure perturbation for (a) the pseudo-incompressible and (b) the modified-compressible infinite atmosphere. Each field is normalized by the absolute maximum value in the compressible case ($0.048\Delta p$). The heating half-width is $a = 100$ km; the half-depth is $d = 5$ km.

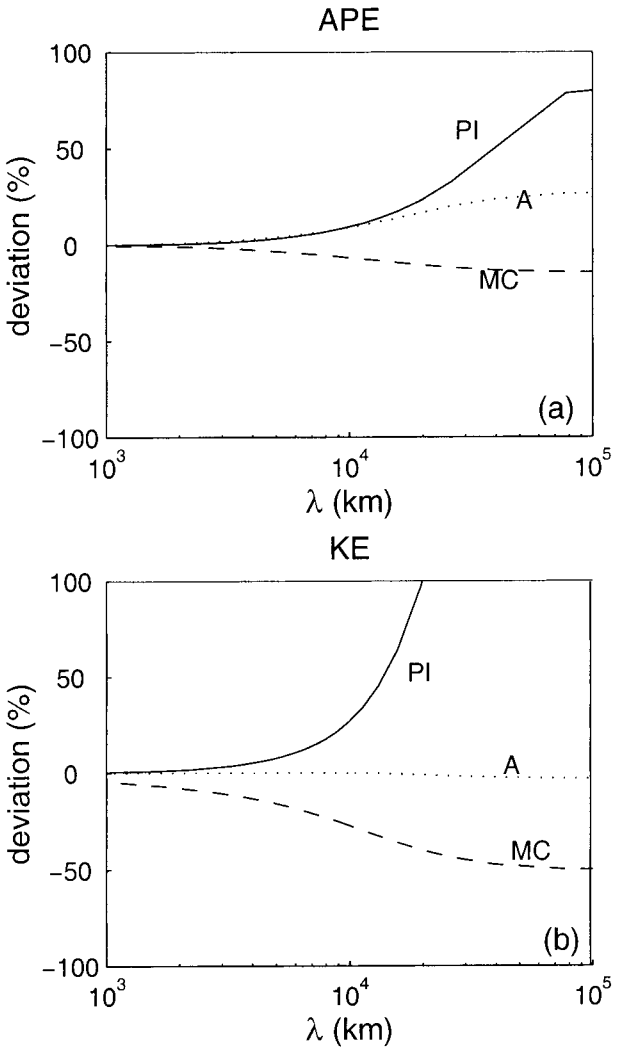


FIG. 11. Percentage deviation of the modified-compressible (MC, dashed lines), pseudo-incompressible (PI, solid lines), and anelastic (A, dotted lines) energetics from the compressible energetics as a function of wavelength. (a) APE and (b) KE.

ance for $t > 0$. In contrast, the modified-compressible balance [$\delta_1 = 0$, $\delta_2 = 1$, $\gamma^* = \gamma$] retains the storage of available elastic energy for $t > 0$. However, there is no initial generation by the heating of available elastic energy, by (4.5), because there is no initial pressure perturbation in this approximation.

Figure 11 presents the steady-state perturbation energetics for the approximate equations as a white noise spectrum. The kinetic and available energies of the anelastic, pseudo-incompressible, and modified-compressible atmospheres are computed as deviations from the compressible values. For example,

$$\delta \mathrm{KE}_{\mathrm{anelastic}}(\%) = 100 \times \frac{(\mathrm{KE}_{\mathrm{anelastic}} - \mathrm{KE}_{\mathrm{compressible}})}{\mathrm{KE}_{\mathrm{compressible}}}. \quad (4.12)$$

The presentation of wave energetics is omitted because this calculation requires complete knowledge of the initial total energy and this energy is different in each atmosphere (see section 4b). The presentation of the available elastic energy is omitted because the approximations either omit its storage or its generation (see Fig. 1). The errors in the anelastic energetics are the smallest, with its kinetic energy being identical to the compressible kinetic energy. The modified-compressible approximation underestimates the kinetic and available potential energy. This behavior reflects the addition of the monopole contribution to the compressible solution that reduces the strength of the upper-level anticyclone where the bulk of the final state energy resides. In contrast, the pseudo-incompressible approximation's overestimation of these energies reflects a stronger upper-level anticyclone. The deviations in the kinetic en-

ergy are particularly sensitive at large scales where the compressible kinetic energy, and hence the denominator in (4.12), tends to zero.

## 5. Discussion

We have presented analytical, initial, and steady-state solutions to a linear hydrostatic and geostrophic adjustment problem in a compressible, stratified atmosphere. An instantaneous heating function with top-hat vertical structure and horizontally decaying spatial structure creates the initial imbalance. The heating produces a pressure, entropy, and potential vorticity disturbance confined to the heated layer, to which the flow fields in turn adjust. Such heating can be used to model a synoptic-scale atmospheric response to an embedded, mesoscale convective cluster, or the linear mesoscale response to an isolated cloud.

The steady-state solutions are obtained from the initial conditions by consideration of potential vorticity conservation. The heating function produces a vertical potential vorticity dipole that uniquely determines the steady state for prescribed vertical boundary conditions. For a warming, the steady state is characterized by an upper-level anticyclone and a low-level cyclone. This low-level, low pressure perturbation in the hydrostatic and geostrophic steady state is a result of a net mass loss in the heated column due to horizontal transport. It is absent from the one-dimensional, hydrostatic adjustment problem (Bannon 1995a).

The amplitudes of the steady-state perturbation fields are dependent on the length scale of the heating. Consider an initial heating with $a = 100$ km, which generates an initial potential temperature anomaly of 10 K. In this case the pressure scale, $\Delta p$, is 29.65 hPa. Then the steady-state fields have maximum values of 1.42 hPa, 6.37 K, 0.0086 kg m$^{-3}$, and 5.8 m s$^{-1}$ for pressure, potential temperature, density, and velocity, respectively. The maximum displacements are 295 m and 58.7 km in the $z$ and $x$ directions, respectively. These values do not change significantly when the heating half-width is on the synoptic scale (e.g., $a = 1000$ km). However, the steady-state perturbations are significantly smaller when the heating half-width is $a = 10$ km. In this case, the fields have maximum values of 0.22 hPa, 1.0 K, 0.0014 kg m$^{-3}$, and 0.92 m s$^{-1}$ for pressure, potential temperature, density, and velocity, respectively. The maximum displacements in this case are 47 m and 9.4 km in the $z$ and $x$ directions, respectively. It is clear that heating produced by a typical mesoscale convective system produces a significant synoptic-scale balanced response. The adjustment to a smaller-scale heating, such as an isolated thunderstorm, is dominated by a wave response.

The effect of vertical boundary conditions has also been considered. The semi-infinite and the finite atmospheres demonstrate several departures from the infinite model. In the infinite atmosphere, the low-level cyclone is narrower and weaker than in the semi-infinite atmosphere. The lower boundary inhibits the vertical expansion of the heated layer while concentrating the strength of the horizontal low-level flow near the boundary. In the finite atmosphere, a rigid lid suppresses the net upward expansion of the heated layer and concentrates the horizontal upper-level flow near the boundary to an even larger extent. Consequently, a smaller fraction of energy is projected onto wave energy in the finite atmosphere. The relative closeness of a boundary can be measured by the ratio of geometric distance to the boundary divided by the Rossby height. Thus the impact of the boundaries is most pronounced at large horizontal wavelengths or when the heating takes place closer to the boundaries. At small horizontal wavelengths, or when the heating takes place sufficiently far away from the boundaries, the solutions are less affected by the choice of boundary condition.

The compressible solution to the hydrostatic and geostrophic adjustment problem has been used to evaluate the anelastic, modified-compressible, and pseudo-incompressible approximations. In the anelastic atmosphere, the initial response to the heating includes an instantaneous acoustic adjustment whose effect is to broaden, weaken, and deepen the initial pressure field relative to the compressible case. In addition, the adjustment produces a rarefaction at the levels of the heating with weak compressions above and below. The steady-state pressure field in the anelastic atmosphere is the same as that for the compressible atmosphere. Then by the hydrostatic and geostrophic relations and the ideal gas law, the density, velocity, and temperature fields are also identical. The anelastic energy conservation equation contains no storage or generation of available elastic energy. In this sense the anelastic approximation is energetically consistent. The steady-state anelastic energetics best model the compressible energetics. Its kinetic energy is identical to the compressible kinetic energy, and its available potential energy contains smaller errors than either the modified-compressible or pseudo-incompressible atmospheres.

The modified-compressible approximation exhibits several shortcomings. Among these is the failure to conserve potential vorticity globally. In this approximation, the heating produces a potential vorticity monopole as well as a dipole. This monopole violates the principle of global potential vorticity conservation and produces an anomalous low pressure field, with an anomalously weak upper-level anticyclone and strong low-level cyclone. In the modified-compressible atmosphere the initial response to the heating occurs at constant pressure. As a consequence, the entropy is manifested as a negative density anomaly. This strong buoyancy forcing would most likely overemphasize the convective nature of the flow evolution. Furthermore, the modified-compressible energetics inconsistently allows for the storage but not the diabatic generation of available elastic energy. The steady-state energetics are characterized by

anomalously small kinetic and potential energy. These errors are largest at large wavelengths, where the acoustic adjustment process is most important and where levels of available elastic energy are largest.

The pseudo-incompressible approximation also exhibits several shortcomings. In the pseudo-incompressible atmosphere the initial response to the heating has a complicated structure including a net flow divergence accomplished by a pulse in the velocity field. The pseudo-incompressible steady-state pressure field contains an anomalously weak and narrow low-level cyclone. These errors are primarily confined to large horizontal wavelength structures. The pseudo-incompressible energetics inconsistently allow for the diabatic generation but not the storage of available elastic energy. By removing elastic energy from the time-dependent energetics, some of the elastic energy initially generated is ambiguously projected onto available potential energy. As is the case with the other approximations, these errors are largest at large horizontal wavelengths.

The modification (Almgren 2000) of the pseudo-incompressible equations to include a time-dependent base state with the assumption that the heating occurs at constant pressure does provide the correct solution for the wavenumber zero case, but it is inapplicable to the more general problem of three-dimensional flow presented here.

The scope of the present investigation has focused on the initial and steady-state response to a prescribed heating in a compressible atmosphere. It provides insight into the problem of hydrostatic and geostrophic adjustment in a realistic compressible atmosphere as well as in several approximate model formulations. However, the transient solution is required to complete the analysis. Buoyancy and acoustic waves account for a considerable fraction of the total energy generated by the heating. Solving the time-dependent problem and partitioning the energetics between the various wave modes requires an analytical technique that solves for each individual wave mode explicitly. Such an investigation is in progress.

*Acknowledgments.* Partial financial support for this work was provided by the National Science Foundation under NSF Grants ATM-9521299 and ATM-9820233.

## APPENDIX A

### Green's Functions Solution of the Steady-State Pressure Equation

The equation governing the compressible, steady-state, transformed pressure is

$$\left(\frac{\partial^2}{\partial z^2} - C^2\right)\hat{P}_f = Be^{z/2H_s}[\delta(z + d) - \delta(z - d)], \quad \text{(A.1)}$$

where $B = (\Delta p/g)H_s S(k, l)$. We apply the principle of superposition such that

$$\hat{P}_f = g_{+d} + g_{-d},$$

where $g_{+d}$ is the solution to (A.1) corresponding to the delta function forcing at $z = +d$, and $g_{-d}$ is the solution corresponding to the forcing at $z = -d$. The solution for the forcing at $z = -d$ satisfies

$$\left(\frac{\partial^2}{\partial z^2} - C^2\right)g_{+d} = Be^{z/2H_s}\delta(z + d), \quad \text{(A.2)}$$

and has the general form

$$g_{-d} = \begin{cases} ae^{-C(z+d)} + be^{C(z+d)}, & z > -d \\ ce^{-C(z+d)} + de^{C(z+d)}, & z \le -d, \end{cases} \quad \text{(A.3)}$$

where $a$, $b$, $c$, and $d$ are constants with respect to $z$. Four conditions are required to determine these constants. The first two conditions are provided by vertical boundary conditions in the upper and lower regions of (A.3). The third condition is that the pressure must be continuous at $z = -d$. The fourth condition follows from an integration of (A.2) about an infinitesimally small region containing $z = -d$. This fourth condition is

$$\lim_{\varepsilon \to 0}\left[\left(\frac{dg_{-d}}{dz}\right)_{-d+\varepsilon} - \left(\frac{dg_{-d}}{dz}\right)_{-d-\varepsilon}\right] = Be^{-d/2H_s}.$$

A similar approach is used to solve for $g_{+d}$.

Table A1 presents the solutions for the various approximations and boundary conditions considered in this paper. In some cases, only $g_{+d}$ is given since $g_{-d}$ can be retrieved from $g_{+d}$ by setting $d \to -d$ and changing the sign of the function.

## APPENDIX B

### Initial Response of a Pseudo-incompressible Atmosphere to an Instantaneous Heating

Consider a pseudo-incompressible atmosphere governed by (2.1a,b,c,d) and (4.1a,b) that is homogeneous in the $y$ direction, with initial condition (2.4), and a heating function of the form

$$\dot{\Theta} = \dot{\Theta}_0\delta(t). \quad \text{(B.1)}$$

The mass conservation equation, from (4.1b) with [$\delta_1 = 1$, $\delta_2 = 0$, $\gamma^* = \gamma$], is

$$\nabla \cdot \mathbf{u}' = \frac{w'}{\gamma H_s} + \frac{\dot{\Theta}}{\theta_s}. \quad \text{(B.2)}$$

Equation (B.2), with (B.1), implies that there must be some delta-function temporal structure in the velocity field. The temporal structure of the fields are generalized as, for example,

$$u' = u_H H(t) + u_\delta\delta(t) + u_{\delta'}\delta'(t) + \cdots, \quad \text{(B.3)}$$

where $H$ is the Heaviside step function, and $\delta'$ is the derivative of the delta function. The higher-order terms (not shown) correspond to higher-order derivatives of the delta function. This generalization no longer allows

TABLE A1. Analytical, steady-state pressure perturbation for the linear hydrostatic and geostrophic adjustment problem described in section 2. Solutions are expressed in the Fourier transform, vertical-coordinate-transform space. The anelastic solution is identical to the compressible solution.

| Description | Solution | Remarks |
|---|---|---|
| Compressible (infinite) | $\hat{P} = \begin{cases} \frac{B}{C}\sinh\left(+Cd + \frac{d}{2H_s}\right)\exp(-Cz), & z > d \\ \frac{B}{C}\sinh\left(+Cz + \frac{d}{2H_s}\right)\exp(-Cd), & -d < z < d \\ \frac{B}{C}\sinh\left(-Cd + \frac{d}{2H_s}\right)\exp(Cz), & z < -d \end{cases}$ | $C^2 = \frac{1}{H_R^2}$ <br> $B = \frac{\Delta p S(k, l)}{\gamma H_s}$ |
| Pseudo-incompressible (infinite) | Same as compressible, except <br> $C^2 = \frac{1}{H_R^2} - \frac{\kappa}{\gamma H_s^2}$ | |
| Modified-compressible (infinite) | Same as compressible plus <br> $\hat{P} = \begin{cases} A\left(1 - \frac{1}{2CH_s}\right)\sinh\left(Cd + \frac{d}{2H_s}\right)\exp(-Cz), & z > d \\ A\left\{\left[-\cosh\left(Cz + \frac{d}{2H_s}\right) - \frac{1}{2CH_s}\sinh\left(Cz + \frac{d}{2H_s}\right)\right]\exp[-Cd]\right. & \\ \quad \left. + \exp(z/2H_s)\right\}, & -d < z < d \\ -A\left(1 + \frac{1}{2CH_s}\right)\sinh\left(-Cd + \frac{d}{2H_s}\right)\exp(Cz), & z < -d \end{cases}$ | $A = -\frac{\Delta p \kappa S(k, l)}{\gamma N_s^2 (k^2 + l^2) H_s^2 / f^2}$ |
| Semi-infinite (compressible) | $g_{+d} = -\frac{B}{2CR} e^{+d/(2H_s)} \begin{cases} (1 - R)e^{-C(z-d)}, & z > +d \\ e^{-C(z-d)} - Re^{+C(z-d)}, & z < +d \end{cases}$ | $R = \frac{\Gamma - C}{\Gamma + C} e^{+2C(D+d)}$ |
| Finite (compressible) | $g_{+d} = -\frac{B}{C(X + XR - E - 1)} e^{+d/(2H_s)} \begin{cases} e^{-C(z-d)} - Ee^{+C(z-d)}, & z > +d \\ X[e^{-C(z-d)} - Re^{+C(z-d)}], & z < +d \end{cases}$ | $R = \frac{\Gamma - C}{\Gamma + C} e^{+2C(D+d)}$ <br> $E = \frac{\Gamma - C}{\Gamma + C} e^{-2C(D-d)}$ <br> $X = \frac{1 - E}{1 - R}$ |

us to claim that the initial velocity field is zero using (2.1a)–(2.1c), nor can we immediately retrieve the initial potential temperature perturbation from (2.1d). We derive a diagnostic equation for the pressure field, using (B.2), (2.1a)–(2.1c), and (4.1a). The result is

$$\left[\frac{\partial^2}{\partial x^2} + \frac{\partial^2}{\partial z^2} + \frac{1}{H_s}\frac{\partial}{\partial z} + \frac{\kappa}{\gamma H_s^2}\right]p' = \rho_s f \frac{\partial v'}{\partial x} + \frac{g}{\theta_s}\frac{\partial}{\partial z}(\rho_s \theta') + \frac{\rho_s}{\theta_s}\frac{\partial \dot{\Theta}}{\partial t}. \quad \text{(B.4)}$$

The nonhomogeneous solution to (B.4) requires the nonhomogeneous solutions for $v$ and $\theta$. The nonhomogeneous pressure solution includes a delta-prime temporal dependence that satisfies

$$\left(\frac{\partial^2}{\partial x^2} + \frac{\partial^2}{\partial z^2} + \frac{1}{H_s}\frac{\partial}{\partial z} + \frac{\kappa}{\gamma H_s^2}\right)p_{\delta'} = \frac{\rho_s \dot{\Theta}_0}{\theta_s}. \quad \text{(B.5)}$$

The pressure is related to the $y$ momentum through the equation

$$\left(\frac{\partial^2}{\partial t^2} + f^2\right)v' = -\frac{f}{\rho_s}\frac{\partial p'}{\partial x}. \quad \text{(B.6)}$$

With the initial condition (2.4), $p_{\delta'}$ implies a step function temporal dependence of $v$ in (B.6):

$$\left(\frac{\partial^2}{\partial t^2} + f^2\right)[v_H H(t)] = -\frac{f}{\rho_s}\frac{\partial [p_{\delta'}\delta'(t)]}{\partial x}. \quad \text{(B.7)}$$

This step function temporal dependence of $v'$ and (2.1b) implies a delta-function temporal dependence of $u'$,

$$v_H = fu_\delta, \tag{B.8}$$

which in turn produces a delta-function dependence in the vertical velocity,

$$\left(\frac{\partial}{\partial z} - \frac{1}{\gamma H_s}\right) w_\delta = -\frac{\partial u_\delta}{\partial x} + \frac{\dot{\Theta}_0}{\theta_s}. \tag{B.9}$$

With the heat equation (2.1d), we may now find the step function temporal dependence of $\theta$. One finds

$$\theta_H = -w_\delta \frac{d\theta_s}{dz} + \dot{\Theta}_0. \tag{B.10}$$

The step function temporal dependence of $p'$ may now be found via the diagnostic pressure equation (B.4) with $\theta_H$ and $v_H$:

$$\left(\frac{\partial^2}{\partial x^2} + \frac{\partial^2}{\partial z^2} + \frac{1}{H_s}\frac{\partial}{\partial z} + \frac{\kappa}{\gamma H_s^2}\right) p_H = \rho_s f \frac{\partial v_H}{\partial x} + \frac{g}{\theta_s}\frac{\partial}{\partial z}(\rho_s \theta_H). \tag{B.11}$$

The step function temporal dependence of $\rho'$ is found using Poisson's equation (4.1a) with $\gamma^* = \gamma$,

$$\frac{\rho_H}{\rho_s} = \frac{p_H}{\gamma p_s} - \frac{\theta_H}{\theta_s}. \tag{B.12}$$

By solving the equations (B.7)–(B.12) sequentially, we can find the initial response corresponding to the instantaneous heating source. An instant after the heating, the particular solution is

$$(u, v, w, p, \theta, \rho)_{t=0^+} = (0, v_H, 0, p_H, \theta_H, \rho_H). \tag{B.13}$$

Thus the pseudo-incompressible atmosphere's initial response to an instantaneous heat source involves the generation of instantaneous vertical and horizontal displacements, accomplished by delta-function vertical and horizontal velocity pulses. Corresponding to these velocity pulses is a pressure field with a temporal dependence given by the derivative of a delta function. The result of the instantaneous displacement is the existence of meridional velocity and density perturbations an instant after the heating.

## REFERENCES


Almgren, A. S., 2000: A new look at the pseudo-incompressible solution to Lamb's problem of hydrostatic adjustment. *J. Atmos. Sci.,* **57,** 995–998.

Arfken, G., 1970: *Mathematical Methods for Physicists.* Academic Press, 815 pp.

Bannon, P. R., 1995a: Hydrostatic adjustment: Lamb's problem. *J. Atmos. Sci.,* **52,** 1744–1752.

——, 1995b: Potential vorticity conservation, hydrostatic adjustment, and the anelastic approximation. *J. Atmos. Sci.,* **52,** 2302–2312.

——, 1996a: Nonlinear hydrostatic adjustment. *J. Atmos. Sci.,* **53,** 3605–3617.

——, 1996b: On the anelastic approximation for a compressible atmosphere. *J. Atmos. Sci.,* **53,** 3618–3628.

Blumen, W., 1972: Geostrophic adjustment. *Rev. Geophys. Space Phys.,* **10,** 485–528.

Bretherton, C. S., 1988: Group velocity and the linear response of stratified fluids to internal heat or mass sources. *J. Atmos. Sci.,* **45,** 81–93.

——, 1993: The nature of adjustment in cumulus cloud fields. *The Physics and Parameterization of Moist Atmospheric Convection,* R. K. Smith, Ed., Kluwer, 63–74.

——, and P. K. Smolarkiewicz, 1989: Gravity waves, compensating subsidence and detrainment around cumulus clouds. *J. Atmos. Sci.,* **46,** 740–759.

Durran, D. R., 1989: Improving the anelastic approximation. *J. Atmos. Sci.,* **46,** 1453–1461.

Gill, A. E., 1982: *Atmosphere–Ocean Dynamics.* Academic Press, 662 pp.

Klemp, J. B., and R. B. Wilhelmson, 1978: The simulation of three-dimensional convective storm dynamics. *J. Atmos. Sci.,* **35,** 1070–1096.

Obukhov, A. M., 1963: On the dynamics of a stratified liquid. *Soviet Phys.-Doklady,* **7,** 682–684.

Raymond, D. J., 1986: Prescribed heating of a stratified atmosphere as a model of moist convection. *J. Atmos. Sci.,* **43,** 1101–1111.

Shutts, G. J., and M. E. B. Gray, 1994: A numerical modeling study of the geostrophic adjustment process following deep convection. *Quart. J. Roy. Meteor. Soc.,* **120,** 1145–1178.